Virtual dielectric waveguide mode description of a high-gain free-electron laser. II. Modeling and numerical simulations

Erik Hemsing,[1] Avraham Gover,[2] and James Rosenzweig[1]
[1]*Particle Beam Physics Laboratory, Department of Physics and Astronomy, University of California Los Angeles, Los Angeles, California 90095, USA*
[2]*Faculty of Engineering, Department of Physical Electronics, Tel-Aviv University, Ramat-Aviv 69978, Tel-Aviv, Israel*
(Received 15 February 2008; published 20 June 2008)

A high-gain free-electron laser is modeled using an expansion of the radiation field in terms of guided Laguerre-Gaussian modes of a virtual dielectric waveguide [E. Hemsing, A. Gover, and J. Rosenzweig, preceding paper, Phys Rev. A **77**, 063830 (2008)]. The radiation profile evolution, power gain, and detuning efficiency characteristics are investigated for seeding with fundamental Gaussian and higher-order Laguerre-Gaussian input modes on a Gaussian *e*-beam in the collective regime. The full wave evolution solution at different seed radiation injection conditions results in determination of the optimal waist size and waist position of the seed radiation beam for maximum power coupling efficiency. Results for guided mode evolution and power gain are shown to be consistent with simulations performed with the code GENESIS 1.3. The amplification and spontaneous generation of FEL radiation with orbital angular momentum is also considered.

DOI: 10.1103/PhysRevA.77.063831 PACS number(s): 42.25.Dd, 41.60.Cr, 42.60.Jf, 42.50.Tx

I. INTRODUCTION

In paper I of this work [1], a set of coupled excitation equations is derived for the slowly growing mode coefficients of the electromagnetic (EM) signal field of a high-gain free-electron laser (FEL) with the effects of longitudinal space-charge waves included. The formulation utilizes an expansion of the time-harmonic EM fields in terms of eigenmodes of a weakly guiding virtual dielectric medium as a mechanism to describe the propagation of radiation guided by the source electron beam (*e*-beam) during exponential gain. The dielectric in the model is referred to as "virtual" since no such external waveguide structure exists in the physical system. The dielectric is imagined to surround the axially propagating *e*-beam and is used as a tool to describe guided waves over many diffracting Rayleigh lengths. This approach is also motivated by the variety of functional forms that can be obtained for the expansion modes, which are determined by the choice of transverse spatial dependence of the dielectric refractive index. This feature is attractive because it permits the freedom to choose a particular basis set in which the coupling and propagation of specific mode structures can be investigated directly. It also makes it possible to study a variety of FEL configurations with arbitrarily shaped *e*-beam current and density cross sections. The expansion modes can also be selected to be close in form to the modes describing the actual FEL system (if they are approximately known, or can be found through iteration), thereby reducing the number of modes required to converge the solution to the correct value and thus boosting the computational efficiency.

Here we focus on a complete orthogonal guided basis set of Laguerre-Gaussian (LG) modes which are of particular interest since they are ubiquitous in descriptions of paraxial wave propagation in circularly symmetric structures. LG modes are related by a simple transformation to Hermite-Gaussian modes, which also satisfy the paraxial wave equation and are common in descriptions of Gaussian optics in systems with rectilinear symmetries. These functions are both available in the guided mode description by choosing a quadratic index medium (QIM) for the form refractive index of the virtual dielectric. This correspondence establishes a useful connection between the guided modes of the FEL and naturally occurring free-space modes, and enables a straightforward examination of the propagation of radiation exiting the undulator, as well as investigation of the coupling characteristics of individual modes in the FEL interaction.

The utility of the LG modes as a convenient FEL modeling basis is further realized in the exploration of specific coupling to higher-order spatial modes. This is of increasing recent interest, particularly due to the development of high-brightness, x-ray FELs in which spatial structure in the transverse intensity distribution can be used for investigations of molecular and atomic scale processes. Hollow modes, in the form of $l>0$ azimuthal LG modes, have recently been a topic of intense research since such modes are known to possess $l\hbar$ units of orbital angular momentum (OAM) per photon as a consequence of an azimuthal component of the linear momentum [2]. For next-generation x-ray FELs that will have the ability to probe the structure of matter on short length and time scales, the generation of such modes may be relevant, since the OAM can be transferred from the photon field to the sample material. Such interactions using conventional laser sources have been previously shown to drive target particles to rotate or orbit the EM beam axis, allowing the possibility of light driven mechanical devices, or the use of torque from photons as a exploratory tool [3]. Recent work has shown that vortex beams that contain OAM modes can be generated using mode-conversion elements placed in the x-ray beam path [4]. However, modern high power x-ray FELs may limit the utility of such extrinsic methods due to damage constraints. For this reason, it is of interest to explore the possibility of generating OAM modes by intrinsic coupling to the source e-beam. In addition, in visible very high average power FELs, it may be advantageous to utilize higher order modes that not only have larger angular spread,

but also have a null in the intensity on-axis. In this way, one greatly eases the problem of thermal loading at the first radiation beam-directing mirror optic downstream of undulator [5,6]. The coupling to these modes, as well as to other higher-order paraxial modes, can be investigated directly by an expansion of the high-gain FEL radiation field in terms of guided LG eigenmodes of a QIM.

In this paper, the coupled excitation equations of the generalized virtual dielectric expansion description are specified and solved for an LG expansion basis. Results are compared to numerical simulations performed using the FEL code GENESIS 1.3 [7]. The radiation fields are examined in the context of differential power gain, spot size evolution, input seed coupling efficiency, detuning efficiency enhancement, and higher-order mode coupling. The LG Gaussian mode basis also provides a straightforward way to examine the accuracy of the single Gaussian mode approximation (SGM) developed in paper I for predicting the supermode r.m.s. spot size. The coupling to, and *in situ* generation of, dominant higher-order LG signal fields that contain OAM at the fundamental operating frequency is also suggested and briefly examined.

II. COUPLED EXCITATION EQUATIONS

In the formulation derived in paper I, the time-harmonic signal fields of the FEL are approximated as dominantly transverse, forward propagating guided waves, and are written as a sum over basis modes with slowly growing coefficient amplitudes

$$\underline{\tilde{E}}_{\perp}(\underline{r}) = \sum_{q} C_q(z)\underline{\tilde{\mathcal{E}}}_{\perp q}(r_{\perp})e^{ik_{zq}z}. \tag{1}$$

The axial wave number for each mode q is taken to be real here and is given by k_{zq}. In a linear model, the e-beam charge density is written as $\mathsf{n}(\underline{r},t)=\mathsf{n}_0 f(r_{\perp})+\mathrm{Re}[\tilde{\mathsf{n}}_1(\underline{r})e^{-i\omega t}]$ where n_0 is the on-axis electron density and $f(r_{\perp})$ is the transverse density profile of the e-beam. The density modulation $\tilde{\mathsf{n}}_1(\underline{r})$ is also expanded in terms of the transverse waveguide eigenmodes

$$\tilde{\mathsf{n}}_1(\underline{r}) = \frac{k\epsilon_0}{e}\sum_{q} B_q(z)\tilde{\mathcal{E}}_{\perp q}(r_{\perp})e^{i(\omega/v_{z_0})z}, \tag{2}$$

where $B_q(z)$ is the slowly varying amplitude of the density modulation with transverse dependence given by the mode function $\tilde{\mathcal{E}}_{\perp q}(r_{\perp})$. This expansion allows the density wave with phase dependence $\omega(z/v_{z_0}-t)$ to be described in terms of the orthogonal field basis functions. The coupled excitation equations for the FEL interaction derived in paper I are

$$\frac{d}{dz}C_q(z) = -i\xi_q\hat{g}_q^* B_q(z)e^{i\theta_q z} - i\sum_{q'}\kappa_{q,q'}^d C_{q'}(z)e^{i(\theta_{q'}-\theta_q)z},$$

$$\frac{d^2}{dz^2}B_q(z) + \theta_p^2\sum_{j}\mathbb{F}_{q,j}B_j(z) = -\frac{1}{\hat{g}_q^*\xi_q}\sum_{q'}Q_{q,q'}C_{q'}(z)e^{-i\theta_{q'}z}, \tag{3}$$

where $\theta_q=\omega/v_{z_0}-(k_{zq}+k_w)$ is the detuning parameter, $\theta_p=\sqrt{e^2\mathsf{n}_0/\gamma\gamma_z^2\epsilon_0 m v_{z_0}^2}$ is the longitudinal plasma wave number on axis in a one-dimensional (1D) model, $\gamma^2=\gamma_z^2(1+K^2/2)$, $\xi_q=Kk^2/4\gamma k_{zq}$, $K=e|\tilde{\mathcal{B}}_{\perp w}|/mck_w$ is the undulator parameter, where $|\tilde{\mathcal{B}}_{\perp w}|$ is the undulator field magnitude, $k_w=2\pi/\lambda_w$ is the undulator wave number and $\hat{g}_q^*=(\hat{e}_z\times\hat{e}_w)\cdot\hat{e}_q^*$ is the polarization alignment factor which measures the relative alignment of the transverse electron motion in the undulator $(\hat{e}_z\times\hat{e}_w)$ with the electric-field mode polarization direction $(\hat{e}_q)$. The EM field mode overlap in the virtual dielectric is given by $\kappa_{q,q'}^d$, the mode coupling coefficient $Q_{q,q'}$ gives the EM field coupling to the wiggling, density-modulated e-beam (or e-beam optical current), and $\mathbb{F}_{q,q'}$ is the beam profile overlap coefficient, which measures the spatial overlap of the e-beam profile with the expansion modes q,q'.

The coupled equations in Eq. (3) fully describe the excitation and dynamic evolution of the signal field and density modulation during the FEL interaction, from the startup period through the high-gain regime. The equations can be solved for an arbitrarily shaped e-beam profile. The effects of longitudinal space charge are also included, assuming that the characteristic transverse e-beam radius is greater than the bunching wavelength $(r_0>\gamma_z\lambda)$ such that fringing fields are neglected. It will be shown here, however, that the equations still adequately describe many of the pertinent features of the FEL when $r_0\sim\gamma_z\lambda$.

III. GUIDED LAGUERRE-GAUSSIAN MODES

The basis eigenmodes used in the expansions of the fields and the density modulation satisfy the dielectric field equation

$$\nabla_{\perp}^2\tilde{\mathcal{E}}_{\perp q}(r_{\perp}) + [n(r_{\perp})^2k^2 - k_{zq}^2]\tilde{\mathcal{E}}_{\perp q}(r_{\perp}) = 0, \tag{4}$$

where the variation in the refractive index is taken to be small in the paraxial approximation $\nabla n(r_{\perp})^2 \ll k$. The spatial dependence of $n(r_{\perp})^2$ in Eq. (4) fully determines the functional form of the expansion basis in the excitation equations. To obtain the desired guided Laguerre-Gaussian modes we choose the refractive index of a QIM, with a specified quadratic spatial dependence of the form

$$n^2(r) = n_0^2 - \left(\frac{r}{z_R}\right)^2, \tag{5}$$

where $z_R=kw_0^2/2$ is the Rayleigh length and w_0 is the characteristic waist size of a transversely Gaussian mode profile. The refractive index on axis n_0 can be set to unity for simplicity. By inserting Eq. (5) into Eq. (4) we obtain guided LG modes which have the form [8–10]

$$\tilde{\mathcal{E}}_{\perp;p,l}(r,\phi) = \tilde{\mathcal{A}}_{p,l}\sqrt{\frac{2}{\pi w_0^2}\frac{p!}{(p+|l|)!}}(-1)^p \times e^{-il\phi}e^{-r^2/w_0^2}\left(\frac{r\sqrt{2}}{w_0}\right)^{|l|}L_p^{|l|}\left(\frac{2r^2}{w_0^2}\right), \tag{6}$$

where $L_p^l(x)=\Sigma_{j=0}^p(p+l)!(-x)^j/j!(p-j)!(l+j)!$ is an associated Laguerre polynomial and $\tilde{\mathcal{A}}_{p,l}$ is a normalization constant such that $\int\int\tilde{\mathcal{E}}_{\perp;p,l}\tilde{\mathcal{E}}^*_{\perp;p',l'}d^2\mathbf{r}_{\perp}=\delta_{p,p'}\delta_{l,l'}|\tilde{\mathcal{A}}_{p,l}|^2$. The

mode index q now takes on two values (p,l) corresponding to the radial and azimuthal mode indices, respectively. (We will use both q and p, l mode indices interchangeably when the multiple indexes are cumbersome). LG modes of this type provide a convenient working basis to model the FEL radiation for geometries that are largely axisymmetric over the interaction length. The field modes in Eq. (6) are identical in the transverse dependence to free-space LG fields that satisfy the paraxial wave equation, when the free-space modes are evaluated at the optical beam waist. The explicit dependence on the Rayleigh length z_R in Eq. (5) defines a specific form for the dielectric profile in which a free-space Laguerre-Gaussian mode with waist size w_0 (defined here as the r.m.s. radius of the Gaussian field profile) will propagate as a guided eigenmode of the virtual dielectric. In this construct, if the guiding features of the e-beam in an FEL during exponential gain are equivalent to those of the QIM, only a single mode in the expansion is required to fully describe the supermode.

The axial wave numbers of the QIM eigenmodes in Eq. (6) differ from the wave numbers of vacuum paraxial modes [10,11]. The waves are modified both in the total wave number by the presence of the homogeneous dielectric contribution kn_0, and by a transverse wave number factor attributed to the guided focusing of the paraxial wave due to the parabolic spatial dependence. Inserting Eq. (5) and (6) into Eq. (4) we obtain the axial wave number associated with each guided mode $k_{zq}=k_{z;p,l}$:

$$k_{z;p,l}^2 = k^2 n_0^2 - \frac{4}{w_0^2}(2p+|l|+1). \tag{7}$$

This describes modal dispersion in the virtual dielectric wherein each mode propagates with an axial phase velocity $\omega/k_{z;p,l}$.

Since the axial field component of the LG modes has a magnitude on the order of λ/w_0 times as large as the associated transverse component, the fields can be considered to be dominantly transverse. For TE modes, we then have a simple relation between the electric and magnetic components: $\tilde{\mathcal{E}}_{\perp q}=-(\omega/k_{zq})\hat{e}_z\times\tilde{\mathcal{B}}_{\perp q}$. The mode power, defined as $\mathcal{P}_q=\frac{1}{2}\mathrm{Re}[\int\int(\tilde{\mathcal{E}}_{\perp q}(r_\perp)\times\tilde{\mathcal{H}}^*_{\perp q}(r_\perp))\cdot\hat{e}_z d^2\mathbf{r}_\perp]$ becomes

$$\mathcal{P}_{p,l} = \frac{k_{z;p,l}}{2\mu_0\omega}|\tilde{\mathcal{A}}_{p,l}|^2. \tag{8}$$

The dielectric mode coupling parameter $\kappa^d_{q,q'}$ in Eq. (3) is defined in general in paper I, and can be evaluated explicitly using the LG basis

$$\kappa^d_{(p,l),(p',l')} = \frac{k^2}{2k_{z;p,l}}\delta_{l,l'}\Bigg[(n_0^2-1)\delta_{p,p'} - \frac{2}{w_0^2k^2} \times \sqrt{\frac{p!\,p'!}{(p+|l|)!\,(p'+|l|)!}}\sum_{j=0}^{p}\sum_{j'=0}^{p'}\binom{p+|l|}{|l|+j} \times\binom{p'+|l|}{|l|+j'}\frac{(-1)^{j+j'+p+p'}(j+j'+|l|+1)!}{j!\,j'!}\Bigg], \tag{9}$$

where $\binom{n}{k}=n!/k!(n-k)!$ is the binomial coefficient. We note that, since $n^2(r)$ is axisymmetric, $\kappa^d_{(p,l),(p',l')}$ vanishes between modes with different azimuthal dependence $(l\neq l')$.

Analytic expressions for the beam profile overlap factor $\mathbb{F}_{q,q'}$ can be found for many functional e-beam profile distributions. Here, the e-beam is assumed to have a fixed, Gaussian transverse profile $f(r_\perp)=\exp(-r^2/r_0^2)$ throughout the interaction length, where r_0 is the r.m.s. radius. In terms of the LG mode expansion basis, $\mathbb{F}_{q,q'}$ becomes

$$\mathbb{F}_{(p,l),(p',l')} = \frac{\tilde{\mathcal{A}}_{p',l'}}{\tilde{\mathcal{A}}_{p,l}}\frac{\delta_{l,l'}(-1)^{p+p'}}{\sqrt{p!\,p'!\,(p+|l|)!\,(p'+|l'|)!}} \times\frac{(p+p'+|l|)!\left(\frac{w_0^2}{2r_0^2}\right)^{p+p'}}{\left(\frac{w_0^2}{2r_0^2}+1\right)^{p+p'+|l|+1}} \times{}_2F_1\left(-p';-p;-p'-p-|l|;1-\left(\frac{2r_0^2}{w_0^2}\right)^2\right), \tag{10}$$

where ${}_2F_1(a;b;c;x)=\Sigma_{n=0}^{\infty}(a)_n(b)_n x^n/(c)_n n!$ is the hypergeometric series and $(a)_n=a(a+1)(a+2)\cdots(a+n-1)$ is the rising factorial. For a single Gaussian EM mode, $\mathbb{F}_{(0,0),(0,0)}=1/(1+\frac{w_0^2}{2r_0^2})$. The e-beam mode coupling parameter $Q_{q,q'}$ is thus

$$Q_{(p,l),(p',l')} = JJ\;\;\theta_p^2\frac{(k_{z;p',l'}+k_w)^2}{8k_{z;p,l}}\left(\frac{K}{\gamma}\right)^2\hat{g}^*_{(p,l)}\hat{g}_{(p',l')}\mathbb{F}_{(p,l),(p',l')}. \tag{11}$$

For modes where the electric-field polarization matches the direction of wiggling motion of the electrons $\hat{g}_{(p,l)}=1$. This "polarization matched" condition is assumed throughout the remainder of this paper.

Equations (9)–(11) are the individual elements of the coupling and overlap terms in the FEL evolution and excitation equations in Eq. (3), solved specifically using the guided LG mode basis. With these terms, the eigensolution of Eq. (3) for the dominant FEL supermode can be found as a superposition of LG modes. The supermode emerges during high-gain and propagates self-similarly and with an exponentially growing field amplitude. Accordingly, the supermode field is defined as $\tilde{\underline{E}}_{\mathrm{SM}}(\underline{r})=e^{ik_{SM}z}\Sigma_{p,l}b_{p,l}\tilde{\underline{\mathcal{E}}}_{p,l}(r_\perp)$ and maintains a fixed transverse profile given by the constant mode coefficients $b_{p,l}$ and the distinct complex wave number $k_{\mathrm{SM}}=k+\widetilde{\delta k}$. The modification of the free-space wave number due the FEL interaction is given by $\widetilde{\delta k}$, and is found from the solution to the supermode matrix equation

$$\{[\underline{\underline{\mathbf{I}}}(\widetilde{\delta k}-\theta)^2-\theta_p^2\underline{\underline{\mathbb{M}}}][\underline{\underline{\mathbf{I}}}\widetilde{\delta k}+\underline{\underline{\kappa}}^d-\underline{\underline{\Delta k}}]+\underline{\underline{Q}}\}\underline{b}=\underline{0}, \tag{12}$$

where the matrix elements of $\underline{\underline{\mathbb{M}}}$ are given by $\mathbb{M}_{q,q'}=(k_{zq'}/k_{zq})\mathbb{F}_{q,q'}$, and the matrices $\underline{\underline{\kappa}}^d$ and $\underline{\underline{Q}}$ are comprised of the elements in Eqs. (9) and (11), respectively. The parameter θ is the detuning in a 1D model and the matrix $\underline{\underline{\Delta k}}$ has elements $(k_{z;p,l}-k)\delta_{p,p'}\delta_{l,l'}$. The dominant mode of the

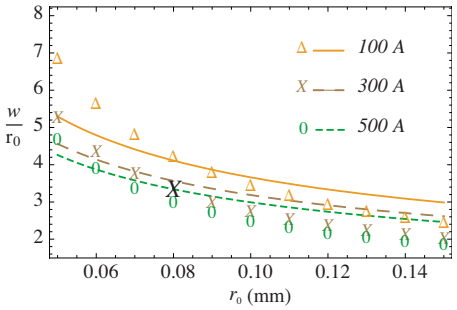

FIG. 1. (Color online) Comparison of the supermode spot size w_{SM}/r_0 identified by markers △, X, and ○, with the predicted size from the SGM approximation w_g/r_0, identified by lines. Three values for the peak *e*-beam current are modeled for VISA parameters, over a range of *e*-beam radii. Markers depict results from solutions to the supermode matrix Eq. (12). At each marker, the detuning in the supermode matrix is set to $\theta=-1/kw_g^2$ in accordance with the SGM formulation, where w_g is given by Eq. (13). The full solutions to Eq. (13) are identified by the colored lines. The large X signifies the usual VISA operating regime, from Table I.

system is given by the solution to the determinant of Eq. (12) with the most negative imaginary value of $\widetilde{\delta k}$. The corresponding 3D power gain length is given by $L_G=(2|\mathrm{Im}\{\widetilde{\delta k}\}|)^{-1}$.

If the system is modeled with only the fundamental Gaussian mode, only the $(p,l)=(0,0)$ elements of the matrices are considered, and Eq. (12) becomes a single algebraic equation. This scenario is explored in paper I and is called the single Gaussian mode approximation or SGM. There, by comparing the difference between axial wave numbers of the guided modes [Eq. (7)] with the axial wave numbers of free-space paraxial modes due to the FEL interaction [10], we obtain a simplified relation between the Gaussian mode spot size w_g, the Gaussian *e*-beam r.m.s. radius r_0 and the 1D coupling gain parameter $Q=(2k_w\rho)^3$,

$$\left(1+\frac{w_g^2}{2r_0^2}\right)\left[1-\frac{2}{kw_g^2Q^{1/3}}\right]^3=1. \tag{13}$$

The solution for w_g can be used as an estimate for the supermode spot size of an FEL that is dominated by the fundamental transverse mode. This technique also provides a useful value for the expansion mode size w_0 that is used in Eq. (6), and is explored for the model FEL in Fig. 1.

IV. NUMERICAL MODELING

To ascertain the character of the FEL system described by the evolution equations in Eq. (3) and the supermode matrix equation in Eq. (12), we use the visible to infrared spontaneous or seeded amplifier (VISA) FEL at Brookhaven National Laboratory as an exploratory model [5,12,13]. The VISA experiment uses a planar undulator geometry and currently operates in self-amplified spontaneous emission (SASE) mode, but will come online shortly also operating as an amplifier of an input radiation signal (seeding). It provides a convenient FEL model for examination of the signal field profile and power evolution in a strong-guiding, diffraction-dominated system ($L_G<z_R<L$). It is also ideal for investigations of LG mode generation since both hollow and spiral transverse EM intensity patterns have been observed during SASE operations, both of which are suggestive of single or multiple interfering OAM modes [14]. The relevant VISA operating parameters are given in Table I.

TABLE I. Seeded VISA parameters.

Parameter	Symbol	Value
Undulator period	λ_w	1.8 cm
Undulator length	L	4 m
Undulator parameter	K	1.26
e-beam relativistic factor	γ_0	123.18
Signal wavelength	λ	1064 nm
e-beam r.m.s. radius	r_0	80 μm
Peak *e*-beam current	I_0	300 A

The VISA FEL is first examined in the ideal case of a pure signal amplifier (SASE effects turned off) to isolate the behavior of the input seed mode as it initiates the FEL interaction and evolves toward the supermode. Ten expansion modes ($p=0-9$, $l=0$) are included in all calculations (unless otherwise noted), and the expansion spot size is taken to be $w_0=3r_0$, in accordance with the best results obtained for efficiency from the SGM approximation in Fig. 2. (Any value of w_0 can be chosen, of course, since it is a free parameter in the expansion. But for a finite number of modes, the greatest efficiency is generally obtained by choosing a value close to that of the eventual FEL eigenmode.) The evolution of the radiation beam is investigated from the seed radiation point to the end of the undulator by solving the coupled mode Eq. (3) for different values w_{s0}, which are the spot sizes the input Gaussian seed modes. The seed radiation beams are introduced coaxially to the undulator and copropagate with the *e*-beam. Figures 3 and 4 follow the longitudinal evolution of the signal field for several input spot sizes, with

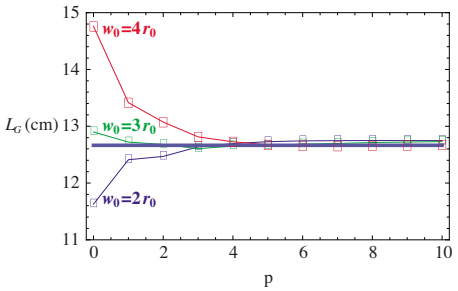

FIG. 2. (Color online) Predicted gain length at resonance for the VISA FEL as a function of the maximum value of the radial mode *p* included in the excitation equations (solid line is from GENESIS). Different values of the expansion waist size w_0 generate a range of values for L_G with only the lowest modes included in the expansion equations, but quickly converge to the correct value as more higher-order modes are added. The best results here are given for $w_0=3r_0$, which is closest to the spot size of the supermode, as given by the full solutions and shown in Figs. 3 and 4.

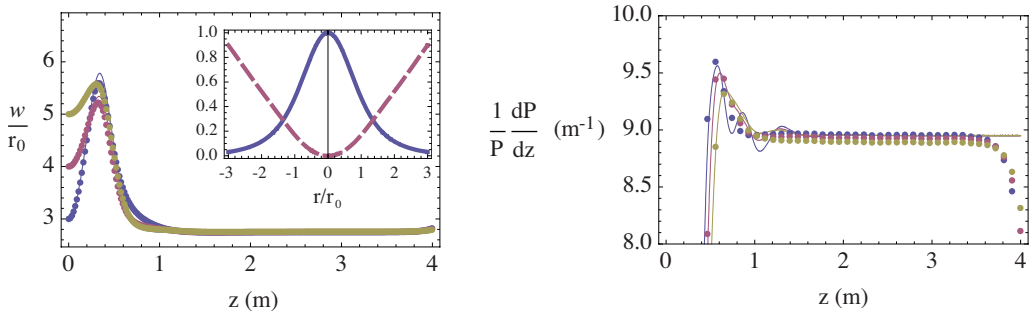

FIG. 3. (Color online) Evolution of the intensity profile (left) and differential power (right) modeled for the VISA FEL operating as a single-pass seed amplifier. Input seed waists $w_{s0}=3r_0,4r_0$, and $5r_0$ of a free-space Gaussian mode are injected coaxially to the e-beam and are positioned at the undulator entrance. The supermode evolves after the fluctuations settle ~1.5 m downstream of injection. Solid lines are solutions to theory from Eq. (3) and points are from GENESIS simulations. The onset of saturation processes is evident near the undulator exit in the GENESIS data, using a $P=0.1$ μW radiation power input, and the shot noise turned off. The effects of longitudinal space-charge waves are neglected. Inset: Normalized transverse intensity (solid) and phase (dashed) profile distribution of the supermode. The vertical axis is in radians.

the Gaussian beam waist located at the undulator entrance $z_0=0$, for the system operating at resonance $\theta=0$. The r.m.s. e-beam radius r_0 is fixed throughout the interaction length, and is set to $r_0=80$ μm as determined by the physical emittance and β-matching constraints for the physical VISA undulator focusing lattice. In Fig. 3 the effects of longitudinal space charge are turned off, and in Fig. 4 they are included for comparison. For each modeled seed injection, the system shows clear dynamic evolution toward the supermode. The input fields are shown to undergo a short period of diffraction during startup before high gain develops. This dynamic behavior is also sensitively recorded in the differential power, where fluctuations are clearly observed before the field eventually settles into fixed gain, fixed profile propagation. This regime of the supermode is also where the effects of longitudinal space-charge waves are most pronounced, identified by the observed reduction in the exponential gain per unit length (Fig. 4). The VISA-FEL is an exemplar of this intermediate regime where the effects of space-charge waves are significant, but not dominant, and must be included in the full calculation for accuracy. In both cases (space-charge on and off), the predicted evolution calculated from the coupled excitation equations in Eq. (3) closely matches the results from simulations performed with GENESIS 1.3 [7], which also includes the effects of fringing in the space-charge fields. This suggests that, even in the VISA regime where $r_0 \sim \gamma_z \lambda$, the "parallel plate capacitor" assumption made for the modulated space-charge fields in the excitation equations still provides reliable results.

In a seeded FEL system, the output power efficiency can be affected, and enhanced, by several design or radiation injection schemes [15]. Experimentally, the simplest method to maximize the available efficiency is to operate off-resonance, i.e., "detune" the system by increasing the e-beam energy (or by increasing the input seed frequency). This effect has been recently observed experimentally [16], and is explored here with the LG dielectric mode expansion for the VISA FEL. Figure 5 shows the dependence of the power gain length L_G on the electron beam energy. It is clear that the shortest gain length is obtained with a positive shift from resonance in the e-beam energy ($\theta<0$).

The relationship between the efficiency and the gain characteristics is also of practical interest for prediction of the optimal spot size and axial waist position of the injected seed mode. Once the supermode is established, the FEL should behave similarly to a single-mode waveguide 1D FEL, but modified by the overall beam profile overlap factor $\mathbb{F}$ that quantifies the departure of the 3D peak gain from the 1D value. The VISA FEL operates in the strongly coupled regime, where the 1D power gain is given by the $G_{1D}=(1/9)e^{\sqrt{3}Q^{1/3}L}$ [17]. In the 3D scenario, the gain is expected to differ from the 1D model, both in the exponential depen-

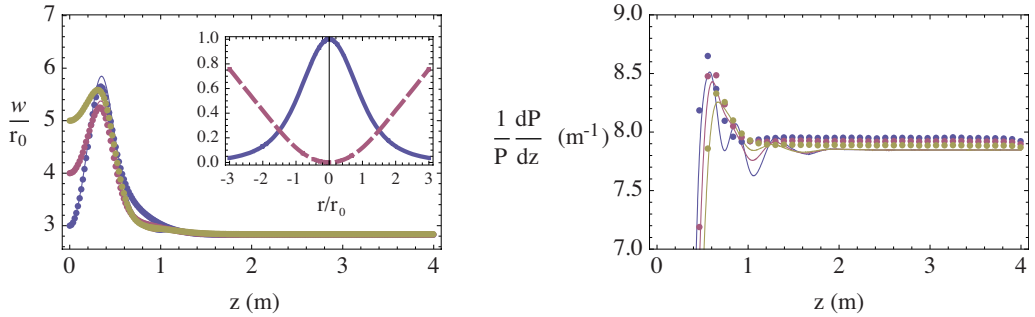

FIG. 4. (Color online) Spot size and power evolution. Running conditions are identical to those in Fig. 3, but with the effects of longitudinal space-charge waves included ($\theta_p=3.22$ m^{-1}). Points indicate results from GENESIS simulations. Inset: Normalized transverse intensity (solid) and phase (dashed) profile distribution of the supermode.

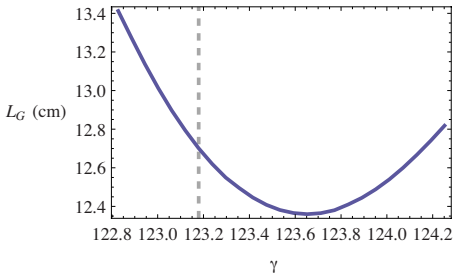

FIG. 5. (Color online) Gain length versus detuning for Gaussian seed input and Gaussian *e*-beam profile. The dashed line indicates resonance ($\gamma=123.18$) for the VISA FEL at 1064 nm. The shortest gain length is obtained for a 0.39% increase in *e*-beam energy factor to $\gamma=123.65$.

dence and in the proportionality. We therefore define a 3D power gain parameter

$$G_{3D} = \frac{1}{9}\eta_{\text{eff}} e^{\mathbb{F}\sqrt{3}Q^{1/3}L}, \tag{14}$$

where η_{eff} is the 3D supermode excitation efficiency. The magnitude of both 3D parameters η_{eff} and $\mathbb{F}$ can be found for a variety of FEL operational schemes in order to ascertain the optimal running conditions. In a seeded FEL, the longitudinal position and waist size of the input seed may have a significant effect on the excitation efficiency of the supermode, particularly for strongly diffracting systems where $z_R \ll L$. Maximum power output is obtained for a proper balance between a small injection spot size to maximize power coupling to the *e*-beam, and a large spot size to minimize power loss from diffraction. Figure 6 shows the dependence of η_{eff} on the longitudinal position and waist size of a Gaussian input seed coupling with a Gaussian *e*-beam for the VISA FEL running parameters. Results indicate that the peak efficiency is obtained when the seed waist is approximately 2–3 times the r.m.s. *e*-beam size, and within the first few 1D gain lengths inside the undulator. By further detuning the system by +0.39% in energy to minimize the gain length (as shown in Fig. 5), the peak available efficiency is increased substantially (Fig. 6, right plot), and the optimal injection occurs when the seed waist is positioned slightly further downstream. It is noted that the optimal waist size for seed injection $w_{s0} \approx 3r_0$ is roughly equal to that of the eventual supermode, as shown in Fig. 3.

The coupling to higher-order paraxial modes, particularly those with $|l|>0$, can be readily explored in the LG expansion basis. By inspection of the mode coupling parameter in Eq. (11), it can be shown that there is no cross-coupling between different azimuthal modes for an axisymmetric Gaussian *e*-beam profile. In addition, none of the $l>0$ modes are excited during seeding with axisymmetric Gaussian input fields, so only the $l=0$ modes contribute to the expansion. It is interesting in this simplified context to consider the amplification of pure azimuthal mode structures for scenarios when it may be necessary to obtain a short pulse, high-peak power OAM mode from the FEL. Since in most cases the fundamental mode usually dominates, generation of a dominant OAM mode can occur if a preferential and significant geometric chirality is intrinsic to the system. Such is the case if, for example, either the seed laser contains nonzero OAM, or if the *e*-beam has a strong helical modulation along the longitudinal axis that will excite a helical phase structure in the radiation field.

Seeding and amplification of pure OAM modes can be examined with the injection of a $l_s>0$ LG mode, where l_s is the azimuthal index of the seed. Results obtained from solving Eq. (3) for both a Gaussian and an $l_s=1$ OAM seed mode are displayed in Fig. 7. The evolution of both inputs shows the development of an eventual FEL eigenmode, both in the intensity profile and in the power gain. It is evident from the plot that there is a decrease in the differential power gain for each increase in the azimuthal mode number of the seed field. This trend continues for seeding with higher order OAM modes and is attributed to the reduction in the effective coupling between the *e*-beam and the field for increasing l values, as given by Eq. (11). This is due, in large part, because the radial profile of modes with $|l_s| \neq 0$ vanishes on axis, and the central null becomes larger transversely for increasing values of l_s. For this reason, it was necessary to detune the system to $\theta=-8.2$ m^{-1} to achieve significant

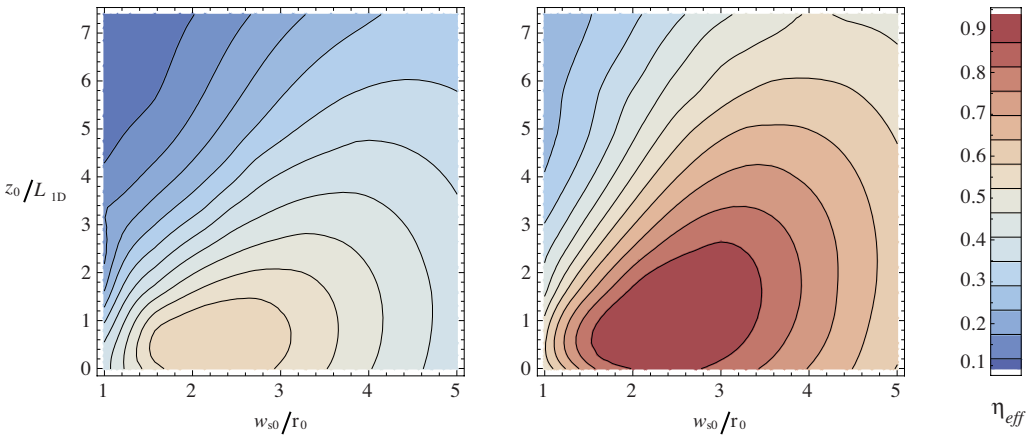

FIG. 6. (Color online) The supermode excitation efficiency η_{eff} for Gaussian seed injection at resonance (left plot, $\theta=0$ m^{-1}) and at a detuning corresponding to the minimum gain length (right, $\theta=-2.7$ m^{-1}). Different longitudinal positions z_0 (vertical) and sizes of the Gaussian seed waist w_{s0} (horizontal) are modeled for the VISA FEL.

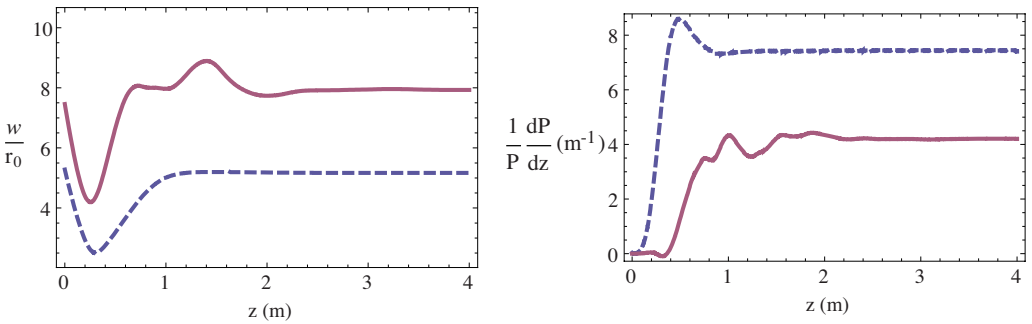

FIG. 7. (Color online) Comparison of signal field propagation for FEL seeding with a pure Gaussian mode (dashed) and a $l=1$ OAM mode (solid), when the effects of plasma space-charge waves are included. Both input seed waists are located $z_0=25$ cm inside the undulator entrance, with the e-beam detuned to $\theta=-8.2$ m^{-1}.

gain. Also, in contrast to seeding with modes with different radial mode numbers p_s (either as pure modes or as a superposition), the eventual output FEL signal fields generated from seeds with different azimuthal mode numbers l_s do not evolve to equal transverse sizes. This is because, for an axisymmetric e-beam profile $f(r_\perp)=f(r)$, the modes with different p values couple to each other, but the different l modes do not. Thus, an excited higher-order radial mode can couple, cascading down toward the fundamental radial mode of the system (usually the Gaussian), but the higher-order l modes are locked. This, combined with the reduced gain length, demonstrates that the character of the final output OAM mode is specifically determined by the input seed field. The l_s mode of the seed is the lone azimuthal mode excited in the FEL interaction for the cold e-beam, and thus defines the fundamental azimuthal mode of the final EM signal field. The system evolves to a state characterized by the features associated with the $l_s>0$ seed mode, including the waist size, gain length, and helical phase evolution. As a result, all of the gain delivered to the radiation field is deposited only into the $l=l_s$ input OAM mode, and a scenario that delivers pure OAM amplification, in the absence of SASE effects, is realized. In the presence of SASE, in order to ignore it's effects, one must seed with power well in excess of SASE startup power, and also take care that the total (potentially higher) gain in the fundamental does not allow this SASE mode to compete with the final power in the desired $l\neq 0$ LG mode.

Generation of coherent OAM light without a seed field input can be investigated in this model by introducing a dominant helical density modulation on the e-beam. The density modulation in Eq. (2) identifies the longitudinal bunching in terms of the expansion mode functions. Nonzero values for $B_{0,0}(0)$ identify a prebunching modulation at the fundamental that can be related to longitudinal shot noise, or a SASE startup scenario. The coefficients $B_{p,l}\neq 0$ for $|l|>0$ describe azimuthal structures in the e-beam, and helical structures occur when $B_{p,l}\neq B_{p,-l}$. Figure 8 shows the transverse intensity and phase at the undulator exit for a solution of the excitation equations with a relative initial density modulation of $B_{0,1}/B_{0,0}=10^5$ (all other coefficients are zero) for VISA. The relative magnitude of each amplitude is determined by iteration, such that the higher-order hollow mode becomes visibly dominant in the transverse intensity profile. It is particularly clear from the phase that the structure is that of a dominant $(p,l)=(0,1)$ LG mode (helical phase evolution), and that the field is gain-guided from the slight appearance of inward curvature near the axis.

It is noted that the amplification of light with OAM should impart a self-consistent orbital momentum to the source e-beam. The effects of this interaction on the overall e-beam dynamics are calculated to be small relative to the dominant FEL interactions considered here, and are neglected.

These results on the amplification of OAM modes at the fundamental frequency of the FEL device suggest that, since an initial bunching modulation at the fundamental mode typically dominates the interaction, amplification of a dominant azimuthal mode requires a dominant azimuthal excitation at startup. We have shown that this can be achieved either by injection of an OAM seed mode with the appropriate intensity amplitude (if available at the operating frequency), or by introduction of the appropriate spatial modulation that is not azimuthally symmetric to the injected beam. The magnitude of these respective initial conditions provides a guideline for required parameters needed to obtain OAM modes in the presence of SASE, and will be explored further in future work.

V. CONCLUSIONS

We have presented a study of the high-gain VISA FEL in the virtual dielectric mode description, specified for a guided Laguerre-Gaussian mode expansion basis, with an emphasis

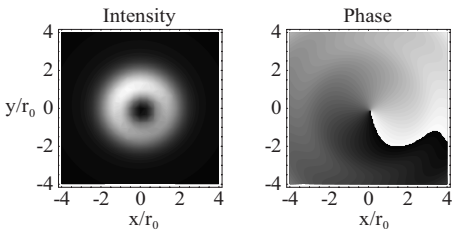

FIG. 8. Radiation intensity and phase at undulator exit, generated by a dominant $(p,l)=(0,1)$ initial helical density modulation in the e-beam. A hollow mode structure is evident in the intensity distribution and is accompanied by a helical azimuthal phase variation.

on OAM mode operation. This interest in OAM modes is driven by the desire to obtain hollow intensity modes that provide power-handling advantages, as well as by applications that depend on the orbital angular momentum in the light pulse. The results of the evolution excitation equations and the supermode matrix equations derived in paper I of this work show good agreement with GENESIS simulations, with the effects of longitudinal space-charge included. The LG mode basis provides a natural description of guided FEL radiation by virtue of its connection to the paraxial modes of free space, and allows the investigation of coupling to modes that contain orbital angular momentum. Results suggest that due to the dominance of the fundamental modes of the typical FEL system, the excitation of a dominant OAM mode requires either an OAM seed, or a significant azimuthal density modulation in the *e*-beam.

ACKNOWLEDGMENTS

This research was supported by grants from the Department of Energy Basic Energy Science Contract No. DOE DE-FG02-07ER46272 and Office of Naval Research Contract No. ONR N00014-06-1-0925.

[1] E. Hemsing, A. Gover, and J. Rosenzweig, preceding paper, Phys. Rev. A **77**, 063830 (2008).
[2] L. Allen, M. W. Beijersbergen, R. J. C. Spreeuw, and J. P. Woerdman, Phys. Rev. A **45**, 8185 (1992).
[3] A. Siegman, *Optical Angular Momentum* (IOP Publishing, London, 2003).
[4] A. G. Peele, P. J. McMahon, D. Paterson, C. Q. Tran, A. P. Mancuso, K. A. Nugent, J. P. Hayes, E. Harvey, B. Lai, and I. McNulty, Opt. Lett. **27**, 1752 (2002).
[5] G. Andonian *et al.*, Phys. Rev. Lett. **95**, 054801 (2005).
[6] W. B. Colson, J. Blau, R. L. Armstead, and P. P. Crooker, Nucl. Instrum. Methods Phys. Res. A **528**, 167 (2004).
[7] S. Reiche, Nucl. Instrum. Methods Phys. Res. A **429**, 243 (1999).
[8] O. Georg, Appl. Opt. **21**, 141 (1982).
[9] L. Yu, W. Huang, M. Huang, Z. Zhu, X. Zeng, and W. Ji, J. Phys. A **31**, 9353 (1998).
[10] A. Yariv, *Optical Electronics in Modern Communications, Oxford Series in Electrical and Computer Engineering* (Oxford University Press, Oxford, 1997).
[11] A. Siegman, *Lasers* (University Science Books, New York, 1986).
[12] A. Tremaine *et al.*, Phys. Rev. Lett. **88**, 204801 (2002).
[13] A. Murokh *et al.*, Phys. Rev. E **67**, 066501 (2003).
[14] G. Andonian, M. P. Dunning, A. Y. Murokh, C. Pellegrini, S. Reiche, J. B. Rosenzweig, M. Babzien, I. Ben-Zvi, and V. Yakimenko, *Proceedings of FEL2006 Conference*, 443–446 (2006).
[15] J. B. Murphy and C. Pellegrini, in *Laser Handbook*, edited by W. Colson, C. Pellegrini, and A. Renieri (North Holland, Amsterdam, 1990), Vol. 6, Chap. 5.
[16] X. J. Wang, T. Watanabe, Y. Shen, R. K. Li, J. B. Murphy, T. Tsang, and H. P. Freund, Appl. Phys. Lett. **91**, 181115 (2007).
[17] E. Jerby and A. Gover, IEEE J. Quantum Electron. **21**, 1041 (1985).